



Published in final edited form as:

Cell Rep. 2016 December 20; 17(12): 3193–3205. doi:10.1016/j.celrep.2016.11.060.

## Blood stage malaria disrupts humoral immunity to the pre-erythrocytic stage circumsporozoite protein

Gladys J. Keitany<sup>1</sup>, Karen S. Kim<sup>1</sup>, Akshay T. Krishnamurthy<sup>1</sup>, Brian D. Hondowicz<sup>1</sup>, William Hahn<sup>1</sup>, Nicholas Dambrauskas<sup>2</sup>, Noah D. Sather<sup>2</sup>, Ashley M. Vaughan<sup>2</sup>, Stefan H.I. Kappe<sup>2</sup>, and Marion Pepper<sup>1,3</sup>

<sup>1</sup>Department of Immunology University of Washington School of Medicine, Seattle, WA 98109

<sup>2</sup>Center for Infectious Disease Research (formerly Seattle Biomedical Research Institute), 307 Westlake Avenue North, No. 500, Seattle, WA 98109

### Summary

Many current malaria vaccines target the pre-erythrocytic stage of infection in the liver. However, in malaria endemic regions, increased blood stage exposure is associated with decreased vaccine efficacy, thereby challenging current vaccine efforts. We hypothesized that pre-erythrocytic humoral immunity is directly disrupted by blood stage infection. To investigate this possibility, we used *Plasmodium*-antigen tetramers to analyze B cells after infection with either late-liver stage arresting parasites or wild type parasites that progress to the blood stage. Our data demonstrate that IgG antibodies against the pre-erythrocytic antigen, circumsporozoite protein (CSP), are generated only in response to the attenuated, but not the wild-type infection. Further analyses revealed that blood stage malaria inhibits CSP-specific germinal center B cell differentiation and modulates chemokine expression. This results in aberrant memory formation and the loss of a rapid secondary B cell response. These data highlight how immunization with attenuated parasites may drive optimal immunity to malaria.

### Graphical abstract

---

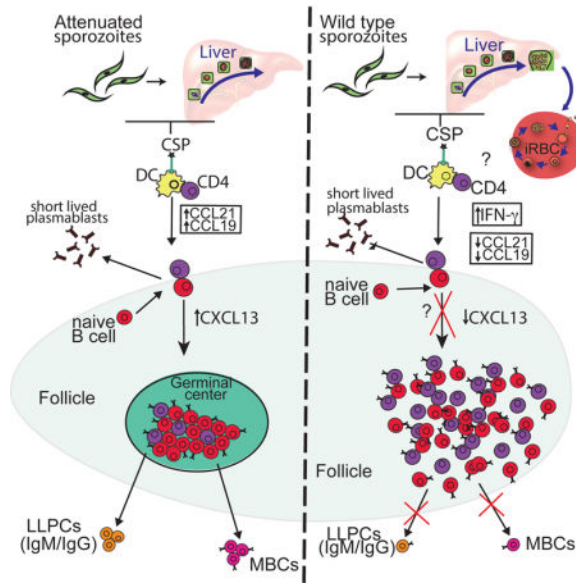
To whom correspondence should be addressed: Dr. Marion Pepper, University of Washington School of Medicine, Department of Immunology, 750 Republican St., Seattle, WA 98109-8059, Telephone: (206) 221-8261, Fax: (206) 616-4274, mpepper@uw.edu.  
<sup>3</sup>Lead contact

**Publisher's Disclaimer:** This is a PDF file of an unedited manuscript that has been accepted for publication. As a service to our customers we are providing this early version of the manuscript. The manuscript will undergo copyediting, typesetting, and review of the resulting proof before it is published in its final citable form. Please note that during the production process errors may be discovered which could affect the content, and all legal disclaimers that apply to the journal pertain.

#### Author Contributions

G.J.K., B.D.H. and M.P. designed experiments and analyzed data. G.J.K., K.S.K and W.H. performed the experiments. A.T.K. developed and optimized the tetramer and provided experimental advice. N.D. and N.D.S provided *PyCSP* and *PyMSP-1<sup>1-19</sup>* protein. A.M.V and S.H.I.K. provided *PyWT* or *PyFabbT* sporozoites and expertise. G.J.K. and M.P. wrote the manuscript and all authors were involved in editing the manuscript.

All authors in these manuscript have no conflict of interest.



## Introduction

Immunization with whole attenuated malaria sporozoites engenders complete sterile protection and robust antibody responses against pre-erythrocytic antigens in both early phase controlled human malaria infection (CHMI) studies with malaria naïve human volunteers, as well as animal studies (Finney et al., 2014b; Keitany et al., 2014; Seder et al., 2013). The most advanced malaria vaccine, RTS,S (based on the pre-erythrocytic stage circumsporozoite protein, CSP), confers modest and short-lived protection (32% efficacy against severe malaria in 5–17-month-old children and around 18% in infants) and anti-CSP antibodies have been correlated with protection (Rts, 2015; Rts et al., 2012; White et al., 2015). In addition, antibodies directed against the pre-erythrocytic stages of infection are slow to develop and found in low frequencies in people living in malaria endemic regions (Del Giudice et al., 1987; Wipasa et al., 2010). Since pre-erythrocytic stage-targeted antibodies can block infection both *in vitro* and *in vivo* and reduce or prevent the parasites progression into symptomatic blood stage infection, it is important to understand why they do not arise effectively in malaria-exposed individuals (Behet et al., 2014; Finney et al., 2014a; Seder et al., 2013).

One possibility is that blood stage infection suppresses immune responses against the pre-erythrocytic stages. Epidemiological studies show that children living in high transmission areas have delayed development of malaria-specific B cells by ELISPOT (Weiss et al., 2010; Wipasa et al., 2010) while children living in low transmission areas with few malaria episodes develop stable malaria specific memory B cells (MBCs) (Wipasa et al., 2010). Studies in murine models have shown that infection with malaria blood stage can lead to inhibition of CD8<sup>+</sup> T cell responses to both malaria specific and other antigens (Khansari et al., 1981; Ocana-Morgner et al., 2003; Ocana-Morgner et al., 2007; Wilson et al., 2006). Furthermore, blood stage infection in rodents can significantly deplete pre-established heterologous long-lived plasma cells (LLPCs) and MBCs resulting in a loss of antibody

responses and increased susceptibility to infection (Banga et al., 2015; Ng et al., 2014; Wykes et al., 2005). A study using the highly inflammatory *Plasmodium berghei ANKA* rodent malaria model showed that severe blood stage infection induced pro-inflammatory responses that inhibited T helper cell differentiation and germinal center (GC) formation (Ryg-Cornejo et al., 2015). Similar observations have been made with other murine parasitic infections such as *Trypanosoma brucei*, which also cause a reduction in pre-established LLPCs and MBCs (Glatman Zaretsky et al., 2012; Radwanska et al., 2008). However, the effect of blood stage infection to antigen specific B cells has not been previously examined and the underlying mechanisms of immune disruption in malaria are not well understood and were the focus of our study.

B cells undergo a tightly regulated program of differentiation into early effector cells and long-lived MBCs that depends largely upon chemokine-guided CD4 T cell-B cell interactions (Zotos and Tarlinton, 2012). Differences in antigen-load, expression of inflammatory cytokines and numerous other factors contribute to the fate of an activated B cell (Kurosaki et al., 2015). Early in the immune response, B cells can form short-lived extrafollicular plasmablasts, or enter a GC where they can undergo somatic hypermutation (SHM) and give rise to class-switched MBCs or plasma cells that produce high-affinity antibodies (Zotos and Tarlinton, 2012). It has recently been recognized that heterogeneous MBC populations can form with different functional capacities, including in response to Plasmodium (Krishnamurthy et al., 2016; Tomayko et al., 2008), suggesting that to truly understand the quality of a humoral response, it is necessary to study both the number and functional identity of antigen-specific B cells.

With accumulating studies suggesting that blood stage malaria has detrimental effects on pre-established antibody responses to different infections, we hypothesized that the blood stage of malaria infection could dysregulate the humoral response to the pre-erythrocytic stage of infection. We tested this hypothesis by comparing antibody responses after infection with *Plasmodium yoelii* wild type (*PyWT*) sporozoites, which complete the pre-erythrocytic stage of infection and establish a blood stage infection, with responses to a genetically attenuated parasite (*Pyfabb/f<sup>-</sup>*) that arrests late in liver stage development and does not cause blood stage infection (Vaughan et al., 2009). Although *PyWT* infection completely abrogated CSP-specific class-switched antibody responses, *Pyfabb/f<sup>-</sup>* infection engendered robust responses. To better understand the underlying mechanisms involved, we developed a B cell tetramer that incorporated the pre-erythrocytic antigen, CSP, allowing us to phenotypically analyze pre-erythrocytic-stage-specific B cells in mice. Blood stage infection by *PyWT* not only induced the early contraction of CSP-specific B cells, but also prevented the development of GC B cells. Moreover, infection with *PyWT* altered the quality of the CSP-specific MBCs, which resulted in an impaired response to a secondary sporozoite challenge. Lastly, we found that blood stage infection affected both inflammatory cytokine and chemokine programs that drive concerted T cell-B cell interactions and are essential for proper B cell differentiation. With significant efforts being made in the design of a pre-erythrocytic stage vaccine that prevents infection in malaria endemic areas, our data raise concerns about administering these vaccines in individuals exposed to blood stage infections.

## Results

### Blood stage infection disrupts antibody responses to pre-erythrocytic antigens

Experimental data in mice suggest that *Plasmodium* blood stage infection can have deleterious effects on humoral immunity to heterologous infection (Banga et al., 2015; Ng et al., 2014). We therefore investigated whether *Plasmodium* blood stages directly affect immunity to the *Plasmodium* pre-erythrocytic antigen, CSP. We took advantage of attenuated *P. yoelii* (*fabb/f<sup>-</sup>*) parasites that lack the endogenous type II fatty acid biosynthesis pathway and, arrest their development as late liver stage schizonts (Vaughan et al., 2009). In consequence, when mice are infected by *Pyfabb/f<sup>-</sup>* sporozoites they do not experience a blood stage infection (Vaughan et al., 2009). In contrast, mice infected with WT sporozoites suffer onset of patent blood stage parasitemia within three days of sporozoite infection with a peak parasitemia reaching an average of 10% by day 14 (Figure S1). This infection is self-resolving and infected red blood cells cannot be detected by day 21. Comparison of *Pyfabb/f<sup>-</sup>* and WT sporozoites allowed us to analyze the B cell response to the pre-erythrocytic-stage antigen CSP, in the presence or absence of a blood stage infection.

To first determine if there are differences in antibody production to CSP in the two different conditions, mice were infected intravenously with 50,000 *PyWT* or *Pyfabb/f<sup>-</sup>* sporozoites and plasma was collected on days 0, 6, 14, 30 and 90. The levels of serum IgM and total IgG against CSP were measured by ELISA. CSP-specific IgM levels were elevated in the serum of both groups of mice, with no significant differences between the two groups six days after infection (Figure 1A). And while CSP-specific IgM antibody levels decreased at days 14 and 30 post-infection, most likely representing a loss of short-lived plasmablasts (Nutt et al., 2015), this loss was more rapid if mice were exposed to a blood stage infection (Figure 1A). Interestingly, a significant decrease in the amount of CSP-specific IgG in the serum was observed in mice infected with *PyWT* compared to *Pyfabb/f<sup>-</sup>* as early as six days after infection and this difference was maintained on both days 14 and 30 post-infection, suggesting that class-switched antibody formation was defective after *PyWT* infection (Figure 1A). This was further supported by ELISA analyses of specific IgG isotypes at all timepoints examined (Figure 1B). To determine whether the diminished antibody responses seen after *PyWT* infection was a global defect or specific to the CSP-response, we also measured antibody responses to *Py* merozoite surface protein 1 (MSP1), expressed primarily in the blood stage of infection (Holder, 1994). Unlike the CSP-specific response, we observed robust expression of MSP1-specific IgM and IgG antibodies in mice infected with *PyWT* sporozoites, while *Pyfabb/f<sup>-</sup>* infected mice lack MSP1-specific responses as expected (Figure 1C).

We next tested if the deleterious effects of blood stage exposure on pre-erythrocytic antibody responses were transient, as previously described for heterologous antibody responses (Ng et al., 2014). To accomplish this, mice were infected with *PyWT* and *Pyfabb/f<sup>-</sup>* and then *PyCSP*- and *PyMSP1*-specific IgM and IgG serum antibody levels were measured 90 days after infection (Figure 1D). In contrast to the transient loss of heterologous antibody previously described, no significant CSP-specific antibody expression was observed in mice

exposed to blood stage infection, while CSP-specific IgG antibodies persisted in *Pyfabb/f* infected animals (Figure 1D). Together these studies demonstrate that blood stage infection abrogates long-term humoral immunity to the pre-erythrocytic stage antigen, CSP.

### Development of a CSP B cell tetramer to track and characterize *Plasmodium*-specific B cells

In an effort to determine how blood stage infection might disrupt B cell differentiation or antibody secreting functions, we utilized previously established techniques (Taylor et al., 2012a) to generate B cell antigen tetramers that identify CSP-specific B cells. Since B cells bind other components of the reagent, including a large population of Phycoerythrin (PE)-specific cells, previously described decoy reagents were also generated to exclude these irrelevant cells (Pape et al., 2011; Taylor et al., 2012a). To facilitate the analysis of small populations of cells, these reagents were used in conjunction with a magnetic bead based tetramer enrichment strategy (Moon et al., 2009).

These reagents and strategies were initially tested on mice immunized with 100 µg of recombinant *PyCSP* in the presence of adjuvant (Figure S2). Spleen and draining lymph nodes were harvested seven days after immunization, single cell suspensions were stained with decoy and then tetramer reagents and anti-PE antibody coated magnetic beads were used to enrich all CSP-specific B cells. Enriched cell fractions containing the population of interest were then surface stained using antibody panels specifically developed to accurately identify all types of CSP-specific B2 B cells and analyzed by flow cytometry (Figure S2). Gating strategies first excluded non-lymphocyte populations, doublets and both CD8<sup>+</sup> and CD4<sup>+</sup> T cells. B2 B cells were subsequently identified by gating on both B220<sup>+</sup> and B220<sup>low</sup>CD138<sup>+</sup> plasma cells (Figure S2A). Within the B2 B cell population, CSP-specific B cells were identified by first excluding Decoy<sup>+</sup> cells and then gating on CSP<sup>+</sup> B cells (Figure S2B and 2A). While approximately ~3000 CSP-specific B cells could be found in a naïve mouse, this number expanded to ~15,000 in CSP-protein immunized mice (Figure S2B and C). More importantly, these cells differentiated into a small percentage of *PyCSP*-specific plasma cells (CSP<sup>+</sup>CD38<sup>low</sup>CD138<sup>+</sup>) and a larger percentage of GC B cells (CSP<sup>+</sup>CD38<sup>low</sup>CD138<sup>-</sup>GL7<sup>+</sup>) unlike their naïve counterparts (Figure S2B). These data demonstrated that our flow-cytometry based technique accurately identified even small numbers of *PyCSP*-specific B cells that could be visualized during the response to CSP.

### Blood stage infection inhibits CSP-specific B cell responses

Our analyses of serum antibody levels revealed that blood stage infection abrogates humoral immune responses to the pre-erythrocytic stage antigen, CSP. To understand if blood stage infection affects the quantity or quality of the response to the pre-erythrocytic stages, we utilized tetramers to determine the kinetics of the CSP-specific B cell response in either attenuated or WT sporozoite infected mice. CSP-specific B cells were enriched from spleens of either uninfected or *PyWT* or *Pyfabb/f* mice infected 6, 14, 30 or 90 days prior. Infection with both *PyWT* and *Pyfabb/f* sporozoites lead to a similar nine-fold expansion of CSP-specific B cells 6 days after infection (28,000 and 27,000, respectively) (Figure 2A and B). Strikingly however, while the expanded CSP-specific B cell population was maintained in the *Pyfabb/f* infected mice, we observed a more rapid decline in the number of CSP-

specific B cells in mice exposed to a WT blood stage infection, such that only 6,000 CSP-specific B cells remained in *PyWT*-infected mice 14 days after infection (Figure 2A and B). Despite a slower contraction in *Pyfabb/f* infected mice, equivalent numbers of CSP<sup>+</sup> MBCs remained in both groups of animals 30 days after infection that were maintained as a stable memory population for at least 90 days after infection (Figure 2A and B). These data demonstrated that exposure to blood-stage infection lead to an equivalent expansion, but a premature contraction of CSP-specific B cells, resulting in equal numbers of CSP-specific MBCs at late time points.

### Exposure to blood stage infection alters the differentiation of CSP-specific B cells

Activation of a B cell through B cell receptor (BCR) binding to antigen in the context of additional co-stimulatory signals and/or interactions with T cells, leads to the development of different B cell fates. B cell fates include antibody-secreting short-lived plasmablasts, GC B cells that undergo somatic hypermutation and affinity maturation, LLPCs and MBCs (Kurosaki et al., 2015). To determine if the premature contraction of the CSP-specific B cell response in *PyWT* infected mice was associated with aberrant differentiation or loss of a specific B cell subset, the phenotype of CSP-specific B cells was examined in our two distinct infection groups. Early arising CSP-specific plasmablasts were identified by the loss of expression of CD38 and increased expression of CD138 (Figure 3A). Large populations of CD38<sup>low</sup> CD138<sup>hi</sup> CSP-specific B cells emerged six days after infection, with no significant differences between *PyWT* and *Pyfabb/f* parasites, (Figure 3A). Interestingly, at day 14 post-infection there is a small, but significantly greater number of CD38<sup>low</sup>CD138<sup>high</sup> cells in the *fabb/f* group, suggesting the slower decline of the plasmablast population in these mice. After short-lived plasmablasts disappear (>30 days after infection), a small population of previously described splenic plasma cells re-emerges in *Pyfabb/f* infected mice, but not mice infected with *PyWT* (Bortnick et al., 2012), (Figure 3A and B). These data demonstrate that exposure to blood stage infection altered the development of CSP-specific B cells and disrupted the formation of splenic LLPCs, which may suggest aberrant GC formation.

Since GC B cells are the precursors of MBCs and LLPCs, we next examined the formation of GC B cells in the same samples (Dups et al., 2014). Germinal center B cell differentiation has been associated with the temporal regulation of both GL7 and CD38. Initially, activated CD38<sup>+</sup>CD138<sup>-</sup> precursors up-regulate GL7 (Taylor et al, 2012a) (Figure 3B). These activated precursor cells can then either down-regulate CD38 as they transform into a GC B cell or alternatively, down-regulate GL7 and become a MBC (Taylor et al., 2012a). At six days post- infection, there is the emergence of a GC B cell population in the *Pyfabb/f* infected mice, but mostly activated precursors in the *PyWT*-infected mice (Figure 3A and 3B). These phenotype persisted at day 14 and at no point did we observe fully differentiated CSP-specific GC B cells in mice that were infected with WT parasites (Figure 3B). These data further support the finding that exposure to blood stage infection affects both the kinetics and quality of the CSP-specific B cells.

Since our antibody data suggested that class-switched IgG antibodies against the blood stage protein MSP1 can form in WT infected mice, we additionally developed a B cell tetramer



against the C-terminus of *PyMSP1* to determine if fully differentiated  $CD38^{-}GL7^{+}$  *MSP1*-specific GC B cells could form. Mice were infected with either *Pyfabb/f* or *PyWT* sporozoites and *MSP1*-specific B cells were enriched and analyzed by flow cytometry on day 14 as described above. In contrast to our observation with the CSP-specific B cells, there was still a  $CD38^{low}CD138^{+}MSP1^{+}$  plasmablast population as well as an ongoing  $CD38^{low}CD138^{-}GL7^{hi}MSP1^{+}$  GC B cell response in *PyWT*, but not *Pyfabb/f* infected mice (Figure S3). These data demonstrate that blood stage infection disrupts the differentiation of B cells responding to pre-erythrocytic antigens such as CSP, but still allows for the development of normal GC responses to blood stage antigens such as *MSP1*. These data further suggest that there is a temporal component to the suppression of humoral immunity since the CSP antigen is only expressed transiently during the pre-erythrocytic stages of infection, while the blood stage antigens are expressed at later time points and for longer duration.

### Blood stage infection changes the phenotype of CSP-specific MBCs

One important potential outcome of an aberrant GC response is the loss of high affinity class-switched MBCs (Zotos and Tarlinton, 2012). Although we did not observe a quantitative difference in the numbers of CSP-specific B cells in either *PyWT* and *Pyfabb/f* infected mice on day 30 (Figure 2B), it was still unclear if there were qualitative differences in the MBCs that form in these two conditions. Recent data has associated the expression of various markers of T cell interactions, such as CD80 and CD73, with MBC functionality (Tomayko et al., 2010). Data from our own lab has confirmed this in B cells responding to *Plasmodium chabaudi* (Krishnamurty et al., 2016). Studies with CD80-deficient mice have showed that CD80 plays an important role in regulating interactions between B and T cells during early and late GC formation and lack of CD80 expression leads to an impaired development of long lived plasma cells (Good-Jacobson et al., 2012). Expression of CD73 is also upregulated in highly functional MBCs and its deletion prevented the development of LLPCs in the bone marrow (Conter et al., 2014). To determine whether blood stage infection perturbed the expression of CD80 and CD73, mice were infected with parasites as described above and CSP-specific B cells were analyzed for surface expression of these phenotypic markers 30 days later. Interestingly, the MBCs from the two groups of mice, despite being numerically equivalent, displayed significant differences in both CD73 and CD80 expression (Figure 4A and B). CSP-specific B cells from *PyWT* infected mice had a fivefold decrease in the percentage of cells that expressed both CD73 and CD80 compared to *Pyfabb/f* infected mice (Figure 4A and B). Since CD80 and CD73 expression can be found on either IgG or IgM MBCs, but not IgD MBCs (Zuccarino-Catania et al., 2014), we also examined the isotype of the CSP-specific MBCs. A significantly higher percentage of CSP-specific MBCs isolated from mice infected with *Pyfabb/f* parasites expressed  $IgM^{+}$  or  $IgM^{-}IgD^{-}$  class-switched (swlg) BCRs than mice infected with *PyWT* parasites, which primarily expressed  $IgM^{-}IgD^{+}$  BCRs (Figure 4C and D). Together these data demonstrate that although there was no difference in the total number of CSP-specific cells between mice infected with WT or attenuated parasites, exposure to blood stage infection reduced the expression of memory markers associated with functionality, and resulted in a largely  $IgD^{+}$  MBC population in *PyWT* infected mice, which are thought to be less responsive to a recall response (Krishnamurty et al., 2016).

### Blood stage infection alters recall responses to a secondary challenge

An effective vaccine will induce the generation of functional MBCs that can mediate long-term immunity. Functional MBCs are characterized by their ability to rapidly produce antibody-secreting cells, generate secondary germinal centers and repopulate memory pools (Tomayko et al., 2008). Interestingly, it has been difficult to induce a long-lived antibody response to pre-erythrocytic antigens in malaria endemic regions (White et al., 2015). The data thus far suggested that perhaps exposure to blood stage infection disrupts the formation of functionally effective CD73<sup>+</sup>CD80<sup>+</sup> CSP-specific MBCs. To test this hypothesis, naïve mice or mice infected 30 days prior with *PyWT* or *Pyfabb/f* were challenged with 50,000 *Pyfabb/f* sporozoites and the numbers and phenotypes of CSP-specific B cells were analyzed three days later. There is no significant increase in CSP-specific B cells in naïve mice, 3 days post-challenge (Figure 5A and B). Importantly, there were significantly higher numbers of CSP-specific B cells three days after challenge in mice primed with *Pyfabb/f* however there was no significant expansion of CSP-specific B cells in mice primed with *PyWT* (Figure 5A and B). Additionally, although there are not significant differences in the numbers of CSP-specific B cells in the two immunized groups prior to rechallenge (Figure 2B and 5B), there are significantly more CSP-specific B cells in the *Pyfabb/f* immunized animals than in *PyWT* primed mice after rechallenge (Figure 5B). Additionally, the numbers of newly formed CSP<sup>+</sup>CD38<sup>-</sup>CD138<sup>+</sup> plasmablasts were significantly higher in rechallenged *Pyfabb/f* mice compared to rechallenged *PyWT* mice (Figure 5C and D). Collectively, these data demonstrate that exposure to blood stage infection changes the intrinsic functionality of CSP-specific MBCs (as measured by proliferation and differentiation) and as a consequence, generates a less effective secondary response.

### Suppression of blood stage restores germinal center response in *PyWT* infected mice

In an effort to determine if the blood stage of infection was directly responsible for aberrant B cell differentiation, it was important to measure CSP-specific B cell responses in *PyWT* infected mice in which the blood stage of infection was eliminated. Mice infected with *PyWT* sporozoites were therefore treated with the anti-malaria drug atovaquone on days three through thirteen after sporozoite infection to inhibit the emergence of a blood stage infection. Treatment with atovaquone effectively eliminated detectable blood stage infection (Figure 6A). Fourteen days after infection, serum was collected from treated and untreated animals and CSP-specific IgG levels were measured by ELISA. Treatment with atovaquone resulted in restored antibody responses to CSP protein (Figure 6B). Furthermore, analyses of CSP-specific B cells in atovaquone treated mice reveal the emergence of fully differentiated germinal center B cells that are significantly greater in number than what is seen in untreated mice (Figure 6C and D). These data demonstrated that the blood stage of infection directly inhibits the germinal center response and therefore humoral immunity to pre-erythrocytic antigens, such as CSP.

### Attenuated parasite infection lacks inflammatory responses associated with disrupted splenic architecture

It has previously been shown that blood stage of malaria infection can disrupt splenic architecture (Cadman et al., 2008). Since the differentiation of functional CD73<sup>+</sup>CD80<sup>+</sup>



MBCs relies upon productive T-B interactions (Taylor et al., 2012b) we next sought to determine if a loss of CSP-specific MBCs in *PyWT* infected mice is associated with this disruption. Upon activation, CD4 T cells and B cells migrate to the T-B border in a tightly regulated, well-orchestrated, chemokine dependent manner (Cyster, 2005). Chemokines that bind to the chemokine receptors CCR7 and CXCR5 mediate this migration towards the T cell zone (also known as the PALS) or B cell zone (also known as the follicle), respectively (Muller et al., 2003). We therefore looked at the positioning of splenic B cells and T cells six and fourteen days after infection with *PyWT* or *Pyfabb/f<sup>-</sup>* parasites, when differences in antibody production are seen (Figure 1B). To accomplish this, spleens from *PyWT* and *Pyfabb/f<sup>-</sup>* infected mice were sectioned and stained with antibodies against IgD, CD4 and GL7 to mark follicles, periarteriolar lymphoid sheath (PALS) and germinal centers respectively (Figure 7A). In *Pyfabb/f<sup>-</sup>* infected mice, well-defined B cell and T cell zones were readily identifiable on day 6 post-infection while in *PyWT* infected mice, CD4 T cells were distributed throughout the follicles with no defined T cell zone (yellow dashed lines, Figure 7A). By day 14 post-infection, GL7<sup>+</sup> germinal centers are fully formed in *Pyfabb/f<sup>-</sup>* infected mice, and are present, but less organized in *PyWT* infected mice (white dashed lines, Figure 7A).

Chemokines such as CCL21, CCL19 and CXCL13 expressed by both hematopoietic and non-hematopoietic compartments orchestrate these migrational programs and are essential for proper germinal center formation (Cyster, 2005). CCL21 and CCL19 recruit CCR7<sup>+</sup>-expressing cells towards the PALS while CXCL13 attracts CXCR5<sup>+</sup> cells into the follicles (Cyster, 2005). Alternatively, expression of the chemokines CXCL9 and CXCL10 can drive CD4 T cells away from the GC and into the interfollicular sinus or splenic medulla, respectively (Groom et al., 2012).

To ask if exposure to the blood stage of infection modulated the expression of these chemokines at a time associated with splenic disruption, the relative levels of *ccl21*, *ccl19*, *cxc113*, *cxc19* and *cxc110* RNA were quantified in spleens by real-time qPCR three, four or six days after infection with *Pyfabb/f<sup>-</sup>* or *PyWT* sporozoites. Two trends were revealed in this experiment. First, *ccl21*, *ccl19* and *cxc113* were significantly diminished in mice infected with *PyWT* parasites compared to those infected with *Pyfabb/f<sup>-</sup>* at various timepoints within the first six days of infection (Figure 7B). Second, both *cxc19* and *cxc110* expression were significantly elevated 3 days after infection with *PyWT* parasites as compared to mice infected with *Pyfabb/f<sup>-</sup>* parasites (Figure 7B).

To further dissect the signals that may contribute to differences in chemokine expression between the two groups, message levels of the chemokine regulatory cytokines lymphotoxin  $\alpha$  and  $\beta$  were measured. In keeping with lower expression of CCL21, at day 3, lymphotoxin  $\alpha$  was also significantly lower in *PyWT* compared to *Pyfabb/f<sup>-</sup>* infected mice (Figure 7C). No significant differences in lymphotoxin  $\beta$  expression were seen (Figure 7c). *Ifi $\gamma$*  message was also compared between the two groups of mice as its expression can lead to the transient down-regulation of CCL21 and CXCL13 (Mueller et al., 2007), as well as the up-regulation of CXCL9 and CXCL10 (Matloubian and Cyster, 2012). Our analysis showed a significant upregulation of *IFN $\gamma$*  three days after infection with *PyWT* parasites as compared to mice infected with *Pyfabb/f<sup>-</sup>* parasites (Figure 7C). Interestingly, release of merozoites from the

liver into the blood and therefore blood stage patency coincides with the timing of differences seen in IFN $\gamma$  levels between the two groups of mice (Figure S1). These data therefore suggest that blood stage exposure induces the expression of various inflammatory chemokines that transiently disrupt T and B cell interactions required for CSP-specific germinal center B cell differentiation.

To further elucidate the signals that drive lymphoid disorganization, we first tested a role for lymphotoxins in this process. It has previously been shown that treatment of mice with a rat anti-mouse lymphotoxin  $\beta$  receptor agonist antibody (clone 4H8, kindly provided by Dr. Carl Ware) restored lymphoid architecture during toxoplasmosis (Zaretsky et al, 2012). Mice infected with *Pyfabb/f* and *PyWT* mice were treated on days 6, 9 and 12 after infection and CSP-specific B cells were examined at day 14 post-infection. Interestingly, in this model, germinal centers were not restored, suggesting other inflammatory mediators or temporal requirements are involved (data not shown).

We next sought to determine if IFN $\gamma$  is the initiating cytokine in this process of germinal center inhibition by the blood stage of infection, we went on to examine CSP-specific B cell differentiation in mice that lacked the ability to signal through their IFN $\gamma$  receptor. At day 14 post *PyWT* infection, there are very few CSP-specific CD38-GL7<sup>+</sup> GC B cells in C57BL/6 mice while there are significantly more CSP-specific CD38-GL7<sup>+</sup> GC B cells in mice that lack IFN $\gamma$  signaling (Figure 7D). Importantly, although there were significant differences between these two groups of mice, the IFN $\gamma$  deficient mice do not fully recapitulate the humoral immune responses seen after infection with attenuated parasites suggesting that other factors are involved in this process and future studies will interrogate these factors.

## Discussion

Several lines of evidence support the idea that immune memory to *Plasmodium* infection is suboptimal, including the purported loss of acquired immunity to infection in individuals who leave malaria endemic regions (Langhorne et al., 2008). Yet, other studies have challenged the notion that all immune memory to malaria is defective and have instead shown that blood-stage specific immune memory can form (Ndungu et al., 2013; Ndungu et al., 2012; Wipasa et al., 2010). For example, in areas of low malaria transmission, long-lived (half-life of ~5–16 years), functional blood-stage specific MBCs were found in a significant proportion of previously exposed individuals, while CSP-specific MBCs were not (Wipasa et al., 2010). To gain a mechanistic understanding of how stage specific memory could form, we used a *Plasmodium*-antigen tetramer reagents in conjunction with either WT or attenuated parasites that are confined to the pre-erythrocytic stages of infection to analyze MBC development.

Our experiments demonstrate that blood stage exposure disrupts the B cell response to the pre-erythrocytic antigen, CSP, potentially explaining why blood stage-specific, but not pre-erythrocytic stage-specific memory can be identified in individuals living in malaria endemic areas. Blood stage infection inhibits CSP-specific antibody responses by altering the development of GC B cells and therefore the quality of the ensuing MBC compartment. We

further showed that the impact of blood stage infection upon pre-erythrocytic B cell responses occurs in a short window of time, early in infection and involves a loss of splenic architecture associated with the upregulation of pro-inflammatory cytokines and the modulation of chemokines that regulate cell migration. Together, these studies emphasize the importance of studying antigen-specific B cell differentiation and function at the single cell level in addition to serum antibody responses.

Our findings may not only explain why natural immunity to pre-erythrocytic antigens is suppressed, but may also explain why it has been so difficult to induce long-term immunity against pre-erythrocytic antigens in malaria endemic regions by vaccination. To date the best vaccination strategy that confers sterile protection in both human and rodent malaria is the use of whole parasites that have been attenuated by irradiation, drug chemoprophylaxis or by gene deletion, such that there is no productive blood stage infection (Belnoue et al., 2004; Bijker et al., 2014; Hoffman et al., 2002; Nussenzweig et al., 1967; Purcell et al., 2008; Roestenberg et al., 2009; Seder et al., 2013; Vaughan et al., 2009). However in malaria endemic regions where blood stage infection is prevalent, vaccine efficacy associated with CSP-specific antibody responses rapidly declines as exposure to blood stage parasites increases (Olotu et al., 2013; White et al., 2015). These data raised the possibility that blood stage infection may represent a potent immune evasion mechanism.

In the present studies, our ability to track the development and function of CSP-specific B cells responding to attenuated or WT sporozoites demonstrated that blood stage exposure directly disrupts the formation of CSP-specific MBCs. Only in the absence of exposure to a blood stage infection, either through infection with *Pyfabb<sup>f</sup>* sporozoites or drug treatment with atovaquone, can robust class-switched CSP-specific germinal center B cells and CD80- and CD73-expressing MBCs form (Figure 4 and 6). Additionally, secondary challenge experiments demonstrated that *PyWT* mice generated fewer CSP-specific B cells and newly formed plasmablasts than *Pyfabb<sup>f</sup>* mice three days after a secondary challenge. These studies therefore demonstrated that blood stage exposure inhibits the development of functional CSP-specific MBCs. Furthermore, these studies highlight the relevance of the recently recognized heterogeneity in MBC subsets and the ability to identify rapid ASC-forming MBCs by the surface markers CD73 and CD80, especially in response to *Plasmodium* (Zuccarino-Catania et al., 2014). Although work from our lab has shown that both *Plasmodium*-blood stage specific IgG<sup>+</sup> and IgM<sup>+</sup> MBCs can be found in human PBMCs from Mali, future studies will need to determine if similar CSP-specific B cells exist and how this compares to vaccine subjects that have only received attenuated parasites (Krishnamurty et al., 2016).

A role for blood stage infection in this disruptive process is further supported by our data demonstrating that inflammatory cytokine and chemokine programs associated with T and B cell interactions differ as soon as a productive blood stage infection is established. Specifically, chemokines that are associated with lymphocyte migration and a productive germinal center response (CCL21, CCL19 and CXCL13) are reduced by WT infection while those that are associated with migration to other lymphoid regions and peripheral tissues (CXCL9 and CXCL10) are enhanced. These differences in chemokine programs between

the two groups of mice are further supported by differences in the inflammatory mediators (LT $\alpha$  and IFN $\gamma$ ) that regulate them.

The Type 1 cytokine, IFN $\gamma$  has been attributed with both protective and pathological roles in murine models of malaria (King and Lamb, 2015). IFN $\gamma$ -deficient mice experience higher parasitemia that takes longer to control after infection with *Plasmodium yoelii* than IFN $\gamma$  sufficient mice (Van der Hyde et al., 1997). However, experimental cerebral malaria induced by infection with *P. berghei* can be mediated by IFN $\gamma$  (Villegas-Mendez et al, 2012) and high levels of inflammation in this fatal infection can also inhibit the global germinal center response (Ryg-Cornejo et al., 2015). Our studies go beyond this finding to demonstrate that even in a less inflammatory infection, the production of IFN $\gamma$  leads to a transient loss of splenic architecture that specifically disrupts long-lived humoral immunity to the pre-erythrocytic antigen, CSP, while allowing the response to blood stage antigens to occur. This is in keeping with other models of Type 1 mediated infection, such as viral infection with LCMV or parasitic infection with *Toxoplasma gondii* in which similar transient disruption of splenic architecture and germinal centers have been described (Glatman Zaretsky et al., 2012; Mueller et al., 2007).

In conclusion, we have developed a system that allows for a detailed examination of the development and function of malaria life-stage specific B cells at the single cell level. Taken together, our data provide a compelling explanation for why individuals living in malaria endemic regions have limited levels of humoral immunity to pre-erythrocytic antigens compared to humoral immunity against blood stage antigens. Disruption of humoral immune responses to pre-erythrocytic antigens insures productive infection, transition to the blood stage and makes transmission to the next individual probable. These data have major implications for why irradiated or genetically attenuated pre-erythrocytic vaccines or sporozoite infection under drug cover may induce optimal immunity to pre-erythrocytic antigens.

## Materials and Methods

### Parasite Growth and Sporozoite Isolation

5–8 week old female Swiss Webster mice were injected with blood from *PyWT*, *PyWT* GFP-luc (Miller et al., 2013) or *PyFabb/f* (Vaughan et al., 2009) infected mice to begin the growth cycle, and used to feed female *A. stephensi* mosquitoes after gametocyte exflagellation. Salivary gland sporozoites were isolated on days 14–17 post infectious blood meal.

### Mice and parasite infections and treatments

5–8 week old female C57BL/6 or IFN- $\gamma$  receptor knock out mice were purchased from the Jackson Laboratory, bred and maintained under specific pathogen free conditions at the University of Washington. Mice are anaesthetized Isoflurane (Piramal healthcare) were infected intravenously (i.v.) via retro-orbital injection with 50,000 *PyWT*, *PyWT* GFP-Luc (Miller et al., 2013), or *PyFabb/f* (Vaughan et al., 2009) sporozoites. To determine parasitemia *PyWT* GFP-Luc were used and parasitemia was determined by flow cytometry

by quantifying GFP expression from days 2–21. Mice that received drug treatments were administered 14.4mg/kg daily from days 2–13. Some mice were treated with 100 µg anti-mouse lymphotoxin β receptor agonist antibody (Clone 4H8) on days 6, 9 and 12 after parasite infection. All experiments were performed in accordance with the University of Washington Institutional Care and Use Committee guidelines.

### Protein expression and Tetramer generation

Recombinant *PyCSP* was cloned, expressed and purified as previously described (Keitany et al., 2014). A 14 kD truncated carboxy terminus of *PyMSP-1* (termed MSP was cloned such that the final expression construct consisted of a tPA secretion signal followed by MSP-1 amino acids 1662–1757 of the native gene, and ending with an 8X histidine/AviTag combination purification tag. Expression and purification was done as previously described (Keitany et al., 2014). Concentrated *PyCSP* and *PyMSP-1* recombinant proteins (>2 mg/mL) were biotinylated using a BirA biotin-protein ligase kit (Avidity, LLC; Aurora, CO), according to manufacturer's instructions. Following the biotinylation step, proteins was purified by gel-filtration using a calibrated Superdex-200 column in HBS-E (10 mM Hepes, pH 7, 150 mM NaCl, 2 mM EDTA) buffer. Biotinylated *PyCSP* and *PyMSP-1* tetramers and decoy reagents were generated as previously described (Taylor et al., 2012a). Briefly biotinylated proteins were incubated with streptavidin-PE at a ratio of 1:4 at room temperature for 30 minutes. The tetramer fraction was centrifuged in a 100KD amicon column (Millipore) to filter out non-tetramerized proteins.

### Cell isolation, Cell enrichment and flow cytometry

Mice were euthanized with CO<sub>2</sub> asphyxiation and the spleens were mashed with the back of a 3cc syringe through Nitex mesh (Amazon.com). Single cell suspensions were stained with PE-AF647 decoy reagent for 10 minutes at room temperature, followed by *PyCSP* or *PyMSP-1* B cell tetramer conjugated to PE for 30 minutes on ice (Taylor et al., 2012a). Cells were then washed and incubated with anti-PE microbeads (Miltenyi Biotec) for 30 minutes. Tetramer positive cells were enriched as previously described (Moon et al., 2007). Enriched cell fraction was stained with surface markers on ice for 20 minutes with antibodies listed on supplemental table 1. All cells were run on the LSR II or Canto RUO (BD) and analyzed using FlowJo software (Treestar).

### ELISA

High binding 96 well ELISA plates (Costar™) were coated with recombinant *PyCSP* or *PyMSP-1* protein at 2µg/mL in calcium bicarbonate/sodium carbonate coating buffer overnight at 4°C. Plates were washed prior to addition of serum 1:400 dilution (Peng et al., 2014) for CSP and MSP in duplicate wells followed by incubation at room temperature for two hours. After washing, HRP-conjugated anti-mouse IgG, IgG1, IgG2c and IgM antibodies (SouthernBiotech) were added at a 1:1000 dilution for 1h at room temperature. Plates were washed and 50µL of TMB substrate (KPL) was added for 2 minutes prior to measuring absorbance at 650 nm.

## Immunofluorescence

Spleens were Isolated from mice 6 and 14 days after infection with *PyFabb/f* or *PyWT* sporozoites and frozen in OCT (TissueTek). 20 µm cryostat sections were fixed in ice-cold acetone for 10 minutes. Sections were stained with rat anti-mouse IgD FITC (BD biosciences), rat anti-mouse CD4 APC (Biolegend), anti-mouse GL7 biotin (ebioscience) and for 1 hour at room temp, followed by Streptavidin, Alexa Fluor® 568 (Thermo scientific) for 1 hour at room temp. Images were acquired using a Nikon Eclipse 90i microscope and NIS Elements BR (Build 738) software was used for the capture of individual images for each channel. Images further analyzed using Adobe Photoshop.

## Quantitative real-time PCR

Whole spleens were harvested and placed in RNA later (Qiagen), stored in -20C till they were ready for processing. Total RNA was extracted using Qiagen RNAeasy kit according to the manufacturer's instructions. CDNA was synthesized using superscript cDNA synthesis kit (Invitrogen). Real-time quantitative RT-PCR was performed for total chemokine and cytokine mRNA using SYBR Green (Applied Biosystems) and detected using a BioRad CFX96 RT system using primers listed in Supplemental table 2.

Quantitative RT- PCR conditions were as follows: 95 °C for 10 min, then 40 cycles of 95 °C for 30 sec, 58 °C for 15 sec and 72 °C for 30. c DNA expression was standardized using the house-keeping gene HPRT. Fold change was calculated relative to the naïve.

## Statistical analysis

Calculations were performed using GraphPad Prism. A Mann Whitney 2-tailed, unpaired *t*-test was used to evaluate statistical significance between groups. A *p* value <0.05 was considered significant.

## Supplementary Material

Refer to Web version on PubMed Central for supplementary material.

## Acknowledgments

We are grateful to William W. Betz and Heather Kain of the Center for Infectious Disease Insectary Facility for mosquito and sporozoite production. *Plasmodium yoelii* MSP1-19 (XL)/VQ1, MRA-48, deposited by DC Kaslow, was obtained from MR4. We thank Carl Ware for anti-LTβR agonist antibody. This work was supported by grants to M.P. (NIH R01AI108626 and R01 AI108626-01A1S1).

## References

- Banga S, Coursen JD, Portugal S, Tran TM, Hancox L, Ongoiba A, Traore B, Doumbo OK, Huang CY, Harty JT, et al. Impact of acute malaria on pre-existing antibodies to viral and vaccine antigens in mice and humans. *PLoS One*. 2015; 10:e0125090. [PubMed: 25919588]
- Behet MC, Foquet L, van Gemert GJ, Bijker EM, Meuleman P, Leroux-Roels G, Hermsen CC, Scholzen A, Sauerwein RW. Sporozoite immunization of human volunteers under chemoprophylaxis induces functional antibodies against pre-erythrocytic stages of *Plasmodium falciparum*. *Malar J*. 2014; 13:136. [PubMed: 24708526]
- Belnoue E, Costa FT, Frankenberg T, Vigario AM, Voza T, Leroy N, Rodrigues MM, Landau I, Snounou G, Renia L. Protective T cell immunity against malaria liver stage after vaccination with



live sporozoites under chloroquine treatment. *J Immunol.* 2004; 172:2487–2495. [PubMed: 14764721]

- Bijker EM, Schats R, Obiero JM, Behet MC, van Gemert GJ, van de Vegte-Bolmer M, Graumans W, van Lieshout L, Bastiaens GJ, Teelen K, et al. Sporozoite immunization of human volunteers under mefloquine prophylaxis is safe, immunogenic and protective: a double-blind randomized controlled clinical trial. *PLoS One.* 2014; 9:e112910. [PubMed: 25396417]
- Bortnick A, Chernova I, Quinn WJ 3rd, Mugnier M, Cancro MP, Allman D. Long-lived bone marrow plasma cells are induced early in response to T cell-independent or T cell-dependent antigens. *J Immunol.* 2012; 188:5389–5396. [PubMed: 22529295]
- Cadman ET, Abdallah AY, Voisine C, Sponaas AM, Corran P, Lamb T, Brown D, Ndungu F, Langhorne J. Alterations of splenic architecture in malaria are induced independently of Toll-like receptors 2, 4, and 9 or MyD88 and may affect antibody affinity. *Infect Immun.* 2008; 76:3924–3931. [PubMed: 18559428]
- Conter LJ, Song E, Shlomchik MJ, Tomayko MM. CD73 expression is dynamically regulated in the germinal center and bone marrow plasma cells are diminished in its absence. *PLoS One.* 2014; 9:e92009. [PubMed: 24664100]
- Cyster JG. Chemokines, sphingosine-1-phosphate, and cell migration in secondary lymphoid organs. *Annu Rev Immunol.* 2005; 23:127–159. [PubMed: 15771568]
- Del Giudice G, Verdini AS, Pinori M, Pessi A, Verhave JP, Tougne C, Ivanoff B, Lambert PH, Engers HD. Detection of human antibodies against *Plasmodium falciparum* sporozoites using synthetic peptides. *Journal of clinical microbiology.* 1987; 25:91–96. [PubMed: 2432083]
- Dups JN, Pepper M, Cockburn IA. Antibody and B cell responses to *Plasmodium* sporozoites. *Frontiers in microbiology.* 2014; 5:625. [PubMed: 25477870]
- Finney OC, Danziger SA, Molina DM, Vignali M, Takagi A, Ji M, Stanisic DI, Siba PM, Liang X, Aitchison JD, et al. Predicting antidiarrhoeal immunity using proteome arrays and sera from children naturally exposed to malaria. *Mol Cell Proteomics.* 2014a; 13:2646–2660. [PubMed: 25023128]
- Finney OC, Keitany GJ, Smithers H, Kaushansky A, Kappe S, Wang R. Immunization with genetically attenuated *P. falciparum* parasites induces long-lived antibodies that efficiently block hepatocyte invasion by sporozoites. *Vaccine.* 2014b; 32:2135–2138. [PubMed: 24582635]
- Glatman Zaretsky A, Silver JS, Siwicki M, Durham A, Ware CF, Hunter CA. Infection with *Toxoplasma gondii* alters lymphotoxin expression associated with changes in splenic architecture. *Infect Immun.* 2012; 80:3602–3610. [PubMed: 22851754]
- Good-Jacobson KL, Song E, Anderson S, Sharpe AH, Shlomchik MJ. CD80 expression on B cells regulates murine T follicular helper development, germinal center B cell survival, and plasma cell generation. *J Immunol.* 2012; 188:4217–4225. [PubMed: 22450810]
- Groom JR, Richmond J, Murooka TT, Sorensen EW, Sung JH, Bankert K, von Andrian UH, Moon JJ, Mempel TR, Luster AD. CXCR3 chemokine receptor-ligand interactions in the lymph node optimize CD4+ T helper 1 cell differentiation. *Immunity.* 2012; 37:1091–1103. [PubMed: 23123063]
- Hoffman SL, Goh LM, Luke TC, Schneider I, Le TP, Doolan DL, Sacci J, de la Vega P, Dowler M, Paul C, et al. Protection of humans against malaria by immunization with radiation-attenuated *Plasmodium falciparum* sporozoites. *J Infect Dis.* 2002; 185:1155–1164. [PubMed: 11930326]
- Holder AA. Proteins on the surface of the malaria parasite and cell invasion. *Parasitology.* 1994; 108(Suppl):S5–18. [PubMed: 8084655]
- Keitany GJ, Sack B, Smithers H, Chen L, Jang IK, Sebastian L, Gupta M, Sather DN, Vignali M, Vaughan AM, et al. Immunization of mice with live-attenuated late liver stage-arresting *Plasmodium yoelii* parasites generates protective antibody responses to preerythrocytic stages of malaria. *Infect Immun.* 2014; 82:5143–5153. [PubMed: 25267837]
- Khansari N, Segre M, Segre D. Immunosuppression in murine malaria: a soluble immunosuppressive factor derived from *Plasmodium berghei*-infected blood. *J Immunol.* 1981; 127:1889–1893. [PubMed: 7028864]
- Krishnamurthy AT, Thouvenel CD, Portugal S, Keitany GJ, Kim KS, Holder A, Crompton PD, Rawlings DJ, Pepper M. Somatically Hypermutated *Plasmodium*-Specific IgM(+) Memory B

- Cells Are Rapid, Plastic, Early Responders upon Malaria Rechallenge. *Immunity*. 2016; 45:402–414. [PubMed: 27473412]
- Kurosaki T, Kometani K, Ise W. Memory B cells. *Nat Rev Immunol*. 2015; 15:149–159. [PubMed: 25677494]
- Langhorne J, Ndungu FM, Sponaas AM, Marsh K. Immunity to malaria: more questions than answers. *Nat Immunol*. 2008; 9:725–732. [PubMed: 18563083]
- Matloubian M, Cyster JG. Th1 cell induction in lymph nodes according to a red-blue chemokine map. *Immunity*. 2012; 37:954–956. [PubMed: 23244716]
- Miller JL, Murray S, Vaughan AM, Harupa A, Sack B, Baldwin M, Crispe IN, Kappe SH. Quantitative bioluminescent imaging of pre-erythrocytic malaria parasite infection using luciferase-expressing *Plasmodium yoelii*. *PLoS One*. 2013; 8:e60820. [PubMed: 23593316]
- Moon JJ, Chu HH, Hataye J, Pagan AJ, Pepper M, McLachlan JB, Zell T, Jenkins MK. Tracking epitope-specific T cells. *Nature protocols*. 2009; 4:565–581. [PubMed: 19373228]
- Moon JJ, Chu HH, Pepper M, McSorley SJ, Jameson SC, Kedl RM, Jenkins MK. Naive CD4(+) T cell frequency varies for different epitopes and predicts repertoire diversity and response magnitude. *Immunity*. 2007; 27:203–213. [PubMed: 17707129]
- Mueller SN, Hosiawa-Meagher KA, Konieczny BT, Sullivan BM, Bachmann MF, Locksley RM, Ahmed R, Matloubian M. Regulation of homeostatic chemokine expression and cell trafficking during immune responses. *Science*. 2007; 317:670–674. [PubMed: 17673664]
- Muller G, Hopken UE, Lipp M. The impact of CCR7 and CXCR5 on lymphoid organ development and systemic immunity. *Immunol Rev*. 2003; 195:117–135. [PubMed: 12969315]
- Ndungu FM, Lundblom K, Rono J, Illingworth J, Eriksson S, Farnert A. Long-lived *Plasmodium falciparum* specific memory B cells in naturally exposed Swedish travelers. *Eur J Immunol*. 2013; 43:2919–2929. [PubMed: 23881859]
- Ndungu FM, Olotu A, Mwacharo J, Nyonda M, Apfeld J, Mramba LK, Fegan GW, Bejon P, Marsh K. Memory B cells are a more reliable archive for historical antimalarial responses than plasma antibodies in no-longer exposed children. *Proc Natl Acad Sci U S A*. 2012; 109:8247–8252. [PubMed: 22566630]
- Ng DH, Skehel JJ, Kassiotis G, Langhorne J. Recovery of an antiviral antibody response following attrition caused by unrelated infection. *PLoS Pathog*. 2014; 10:e1003843. [PubMed: 24391499]
- Nussenzweig RS, Vanderberg J, Most H, Orton C. Protective immunity produced by the injection of x-irradiated sporozoites of *Plasmodium berghei*. *Nature*. 1967; 216:160–162. [PubMed: 6057225]
- Nutt SL, Hodgkin PD, Tarlinton DM, Corcoran LM. The generation of antibody-secreting plasma cells. *Nat Rev Immunol*. 2015; 15:160–171. [PubMed: 25698678]
- Ocana-Morgner C, Mota MM, Rodriguez A. Malaria blood stage suppression of liver stage immunity by dendritic cells. *J Exp Med*. 2003; 197:143–151. [PubMed: 12538654]
- Ocana-Morgner C, Wong KA, Lega F, Dotor J, Borrás-Cuesta F, Rodriguez A. Role of TGF- $\beta$  and PGE2 in T cell responses during *Plasmodium yoelii* infection. *Eur J Immunol*. 2007; 37:1562–1574. [PubMed: 17474154]
- Olotu A, Fegan G, Wambua J, Nyangweso G, Awuondo KO, Leach A, Lievens M, Leboulleux D, Njuguna P, Peshu N, et al. Four-year efficacy of RTS,S/AS01E and its interaction with malaria exposure. *N Engl J Med*. 2013; 368:1111–1120. [PubMed: 23514288]
- Pape KA, Taylor JJ, Maul RW, Gearhart PJ, Jenkins MK. Different B cell populations mediate early and late memory during an endogenous immune response. *Science*. 2011; 331:1203–1207. [PubMed: 21310965]
- Purcell LA, Yanow SK, Lee M, Spithill TW, Rodriguez A. Chemical attenuation of *Plasmodium berghei* sporozoites induces sterile immunity in mice. *Infect Immun*. 2008; 76:1193–1199. [PubMed: 18174336]
- Radwanska M, Guirnalda P, De Trez C, Ryffel B, Black S, Magez S. Trypanosomiasis-induced B cell apoptosis results in loss of protective anti-parasite antibody responses and abolishment of vaccine-induced memory responses. *PLoS Pathog*. 2008; 4:e1000078. [PubMed: 18516300]
- Roestenberg M, McCall M, Hopman J, Wiersma J, Luty AJ, van Gemert GJ, van de Vegte-Bolmer M, van Schaijk B, Teelen K, Arens T, et al. Protection against a malaria challenge by sporozoite inoculation. *N Engl J Med*. 2009; 361:468–477. [PubMed: 19641203]

- Rts SCTP. Efficacy and safety of RTS,S/AS01 malaria vaccine with or without a booster dose in infants and children in Africa: final results of a phase 3, individually randomised, controlled trial. *Lancet*. 2015; 386:31–45. [PubMed: 25913272]
- Rts SCTP, Agnandji ST, Lell B, Fernandes JF, Abossolo BP, Methogo BG, Kabwende AL, Adegnika AA, Mordmuller B, Issifou S, et al. A phase 3 trial of RTS,S/AS01 malaria vaccine in African infants. *N Engl J Med*. 2012; 367:2284–2295. [PubMed: 23136909]
- Ryg-Cornejo V, Ioannidis LJ, Ly A, Chiu CY, Tellier J, Hill DL, Preston SP, Pellegrini M, Yu D, Nutt SL, et al. Severe Malaria Infections Impair Germinal Center Responses by Inhibiting T Follicular Helper Cell Differentiation. *Cell Rep*. 2015
- Seder RA, Chang LJ, Enama ME, Zephir KL, Sarwar UN, Gordon IJ, Holman LA, James ER, Billingsley PF, Gunasekera A, et al. Protection against malaria by intravenous immunization with a nonreplicating sporozoite vaccine. *Science*. 2013; 341:1359–1365. [PubMed: 23929949]
- Taylor JJ, Martinez RJ, Titcombe PJ, Barsness LO, Thomas SR, Zhang N, Katzman SD, Jenkins MK, Mueller DL. Deletion and anergy of polyclonal B cells specific for ubiquitous membrane-bound self-antigen. *J Exp Med*. 2012a; 209:2065–2077. [PubMed: 23071255]
- Taylor JJ, Pape KA, Jenkins MK. A germinal center-independent pathway generates unswitched memory B cells early in the primary response. *J Exp Med*. 2012b; 209:597–606. [PubMed: 22370719]
- Tomayko MM, Anderson SM, Brayton CE, Sadanand S, Steinel NC, Behrens TW, Shlomchik MJ. Systematic comparison of gene expression between murine memory and naive B cells demonstrates that memory B cells have unique signaling capabilities. *J Immunol*. 2008; 181:27–38. [PubMed: 18566367]
- Tomayko MM, Steinel NC, Anderson SM, Shlomchik MJ. Cutting edge: Hierarchy of maturity of murine memory B cell subsets. *J Immunol*. 2010; 185:7146–7150. [PubMed: 21078902]
- Vaughan AM, O'Neill MT, Tarun AS, Camargo N, Phuong TM, Aly AS, Cowman AF, Kappe SH. Type II fatty acid synthesis is essential only for malaria parasite late liver stage development. *Cell Microbiol*. 2009; 11:506–520. [PubMed: 19068099]
- Weiss GE, Traore B, Kayentao K, Ongoiba A, Doumbo S, Doumtable D, Kone Y, Dia S, Guindo A, Traore A, et al. The Plasmodium falciparum-specific human memory B cell compartment expands gradually with repeated malaria infections. *PLoS Pathog*. 2010; 6:e1000912. [PubMed: 20502681]
- White MT, Verity R, Griffin JT, Asante KP, Owusu-Agyei S, Greenwood B, Drakeley C, Gesase S, Lusingu J, Ansong D, et al. Immunogenicity of the RTS,S/AS01 malaria vaccine and implications for duration of vaccine efficacy: secondary analysis of data from a phase 3 randomised controlled trial. *The Lancet Infectious diseases*. 2015; 15:1450–1458. [PubMed: 26342424]
- Wilson NS, Behrens GM, Lundie RJ, Smith CM, Waithman J, Young L, Forehan SP, Mount A, Steptoe RJ, Shortman KD, et al. Systemic activation of dendritic cells by Toll-like receptor ligands or malaria infection impairs cross-presentation and antiviral immunity. *Nat Immunol*. 2006; 7:165–172. [PubMed: 16415871]
- Wipasa J, Suphavilai C, Okell LC, Cook J, Corran PH, Thaikla K, Liwisaeree W, Riley EM, Hafalla JC. Long-lived antibody and B Cell memory responses to the human malaria parasites, Plasmodium falciparum and Plasmodium vivax. *PLoS Pathog*. 2010; 6:e1000770. [PubMed: 20174609]
- Wykes MN, Zhou YH, Liu XQ, Good MF. Plasmodium yoelii can ablate vaccine-induced long-term protection in mice. *J Immunol*. 2005; 175:2510–2516. [PubMed: 16081823]
- Zotos D, Tarlinton DM. Determining germinal centre B cell fate. *Trends Immunol*. 2012; 33:281–288. [PubMed: 22595532]
- Zuccarino-Catania GV, Sadanand S, Weisel FJ, Tomayko MM, Meng H, Kleinstein SH, Good-Jacobson KL, Shlomchik MJ. CD80 and PD-L2 define functionally distinct memory B cell subsets that are independent of antibody isotype. *Nat Immunol*. 2014; 15:631–637. [PubMed: 24880458]

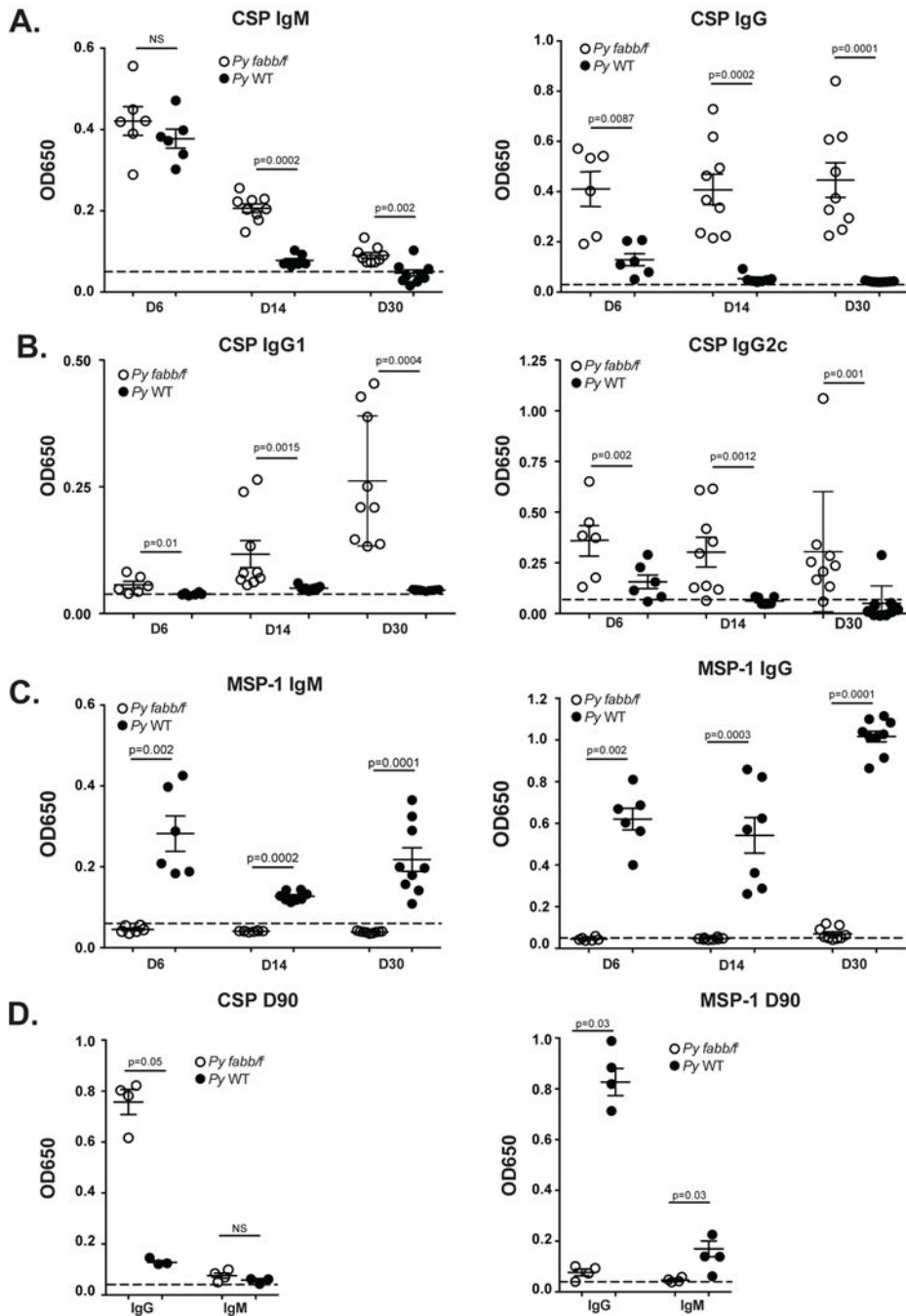


**Figure 1. Infection with *P. yoelii* blood stages abrogates antibody response to pre-erythrocytic antigen**

C57BL/6 mice ( $n=6-9$  mice) were infected with 50,000 *Pyfabbf* (open circles) or *PyWT* (closed circles) sporozoites. Serum was collected 6, 14, and 30 days after infection and was analyzed for the presence of (A) anti-*PyCSP* IgM (left panel), *PyCSP* IgG (right panel), (B) *PyCSP* IgG1 (left panel), and *PyCSP* IgG2c (right panel) and (C) anti-*PyMSP1* IgM (left panel) and IgG (right panel). (D) Serum collected from memory mice ( $n=3-4$ ) on day 90 was also analyzed for the presence of IgM and IgG against *PyCSP* (left panel) and *PyMSP1* (right panel). See also figure S1.

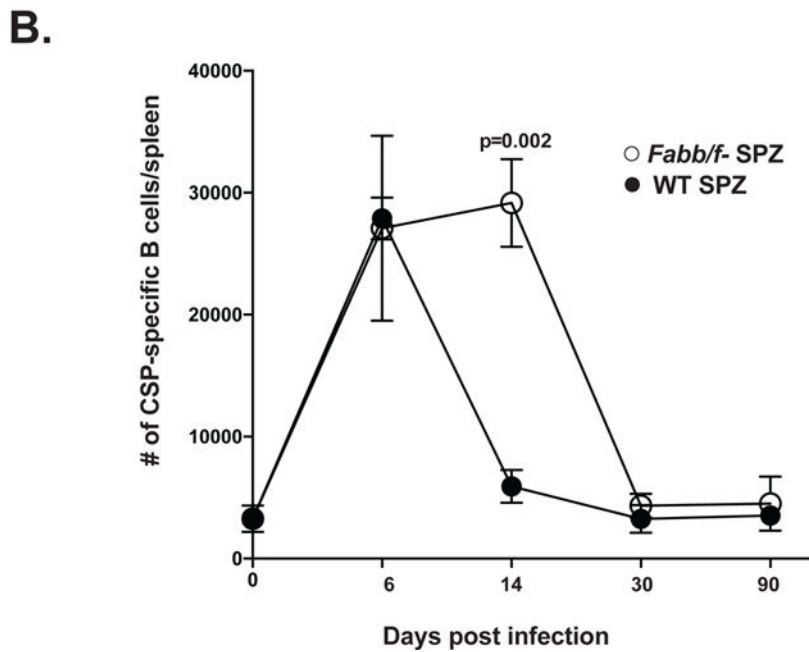
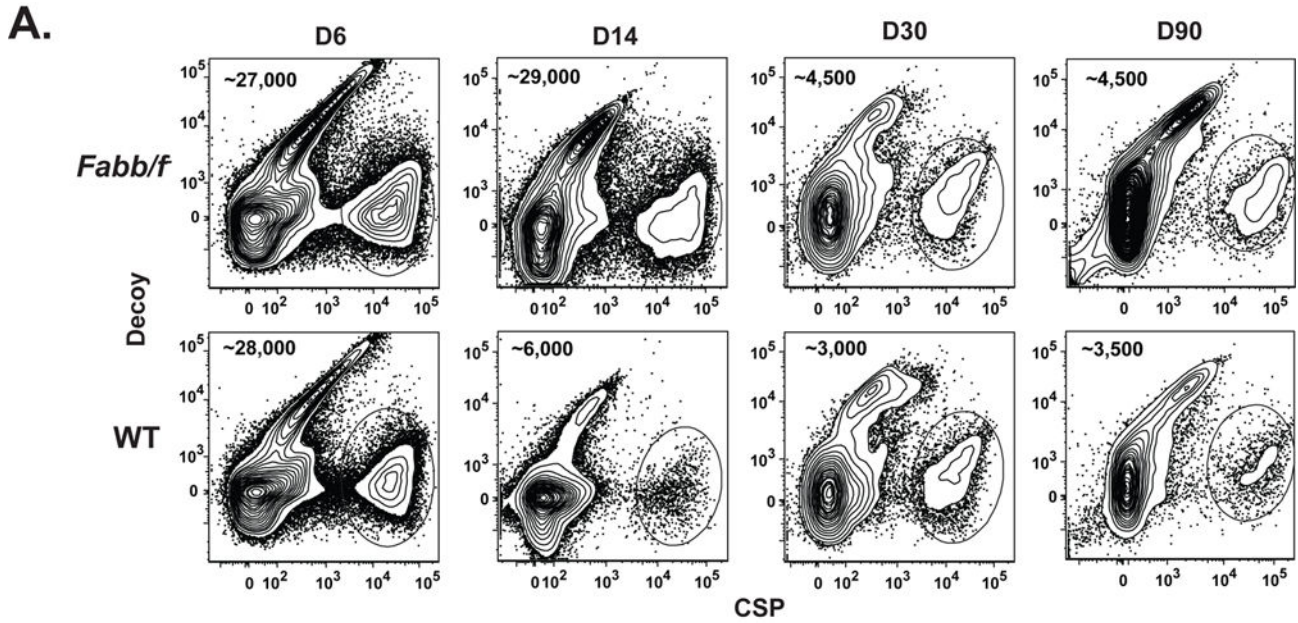


**Figure 2. Kinetics of PyCSP-specific B cells**  
 C57BL/6 mice were infected with *Pyfabb/f* or *PyWT*. Spleens were isolated and *PyCSP*-specific B cells were enriched after 6,14, 30 or 90 days post-infection. (A) Representative flow cytometry plots of spleen B cells from *Pyfabb/f* or *PyWT* infected mice after staining CSP tetramer enrichment with anti-PE magnetic beads and staining for flow cytometry as described in Figure S2. *PyCSP* specific B cells were identified as B220<sup>+</sup>CD138<sup>+</sup> Decoy<sup>-</sup>CSP<sup>+</sup>. (B) Kinetics of CSP specific B cells isolated from spleens of *Pyfabb/f* (open circles) or *PyWT* infected mice.(black circles). Data were compiled from two to three

separate experiments with 3–6 mice per time point. Error bars represent standard deviation (SD). See also figure S2.

Author Manuscript

Author Manuscript

Author Manuscript

Author Manuscript



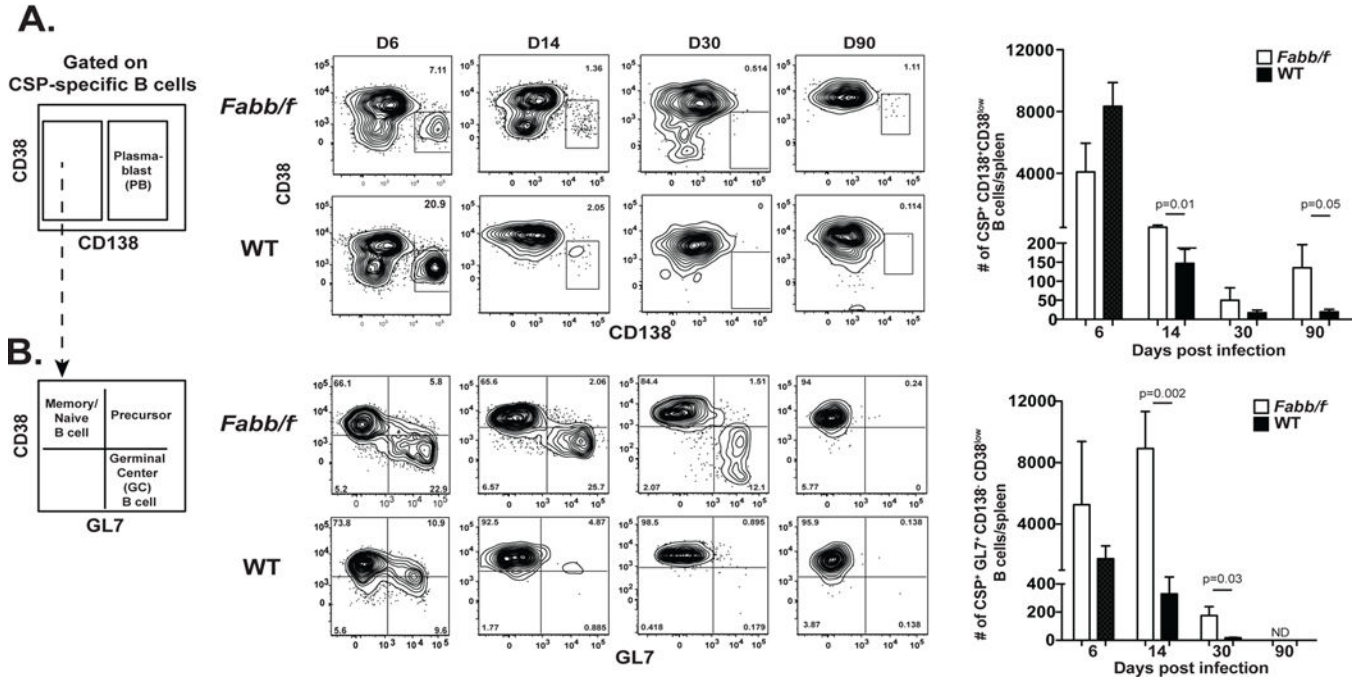


**Figure 3. Blood stage infection alters differentiation of CSP-specific B cells**  
 (A, left) Splenocytes were isolated from *Pyfabb/f* or *PyWT* infected mice harvested on day 6, 14, 30 and 90 and analyzed by flow cytometry for CSP<sup>+</sup>CD38<sup>low</sup> CD138<sup>hi</sup> plasmablasts. (A, right) Absolute number of CSP-specific CD38<sup>low</sup> CD138<sup>hi</sup> cells. (B, left) Splenocytes from *Pyfabb/f* or *PyWT* infected mice were analyzed for CSP<sup>+</sup>CD38<sup>low</sup> CD138<sup>-</sup> GL7<sup>hi</sup> germinal center B cells, on days 6, 14, 30 and 90 by flow cytometry. (B, right) Absolute numbers of CSP<sup>+</sup>CD38<sup>low</sup> CD138<sup>-</sup> GL7<sup>hi</sup> cells. Results are representative of 2–3 independent experiments with 3–6 mice in each. Error bars represent SD. See also figure S3.

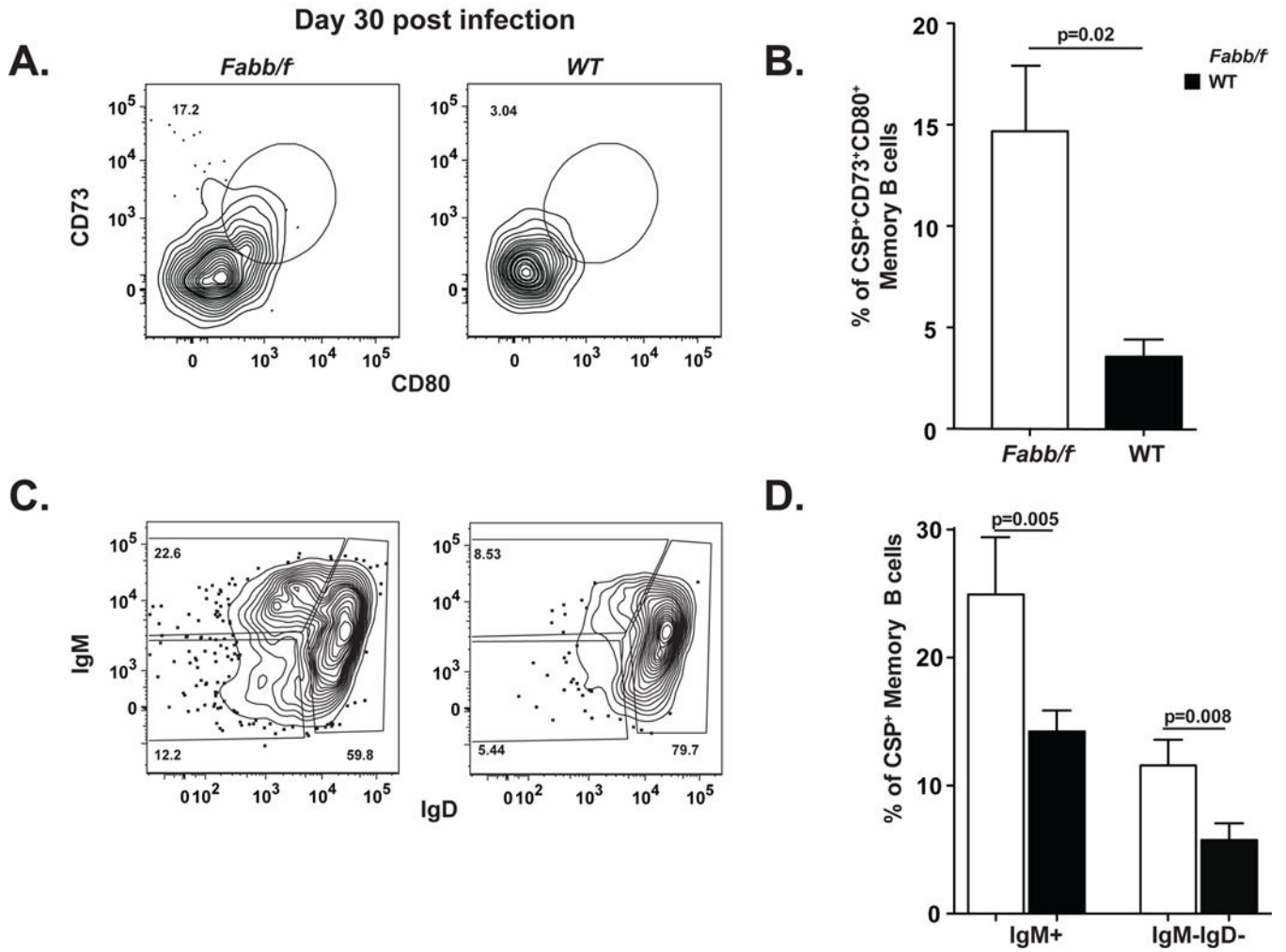


**Figure 4. Blood stage infection compromises the development of CSP-specific memory B cells**  
 (A) Representative plots of CSP-specific memory B cells ( $PyCSP^+CD138^-GL7^-CD38^{high}$ ) stained with CD73 and CD80 30 days post-infection. (B) Summary of data presented in A. (C) Representative plots of  $PyCSP^+$  memory B cells stained with IgD<sup>+</sup> and IgM<sup>+</sup> 30 days post infection (D) Percent of  $PyCSP^+$ -specific memory B cells that are IgM<sup>+</sup> or IgM<sup>-</sup>IgD<sup>-</sup>. Results represent data from at least 2–4 independent experiments with 4–8 mice total. Error bars represent SD.

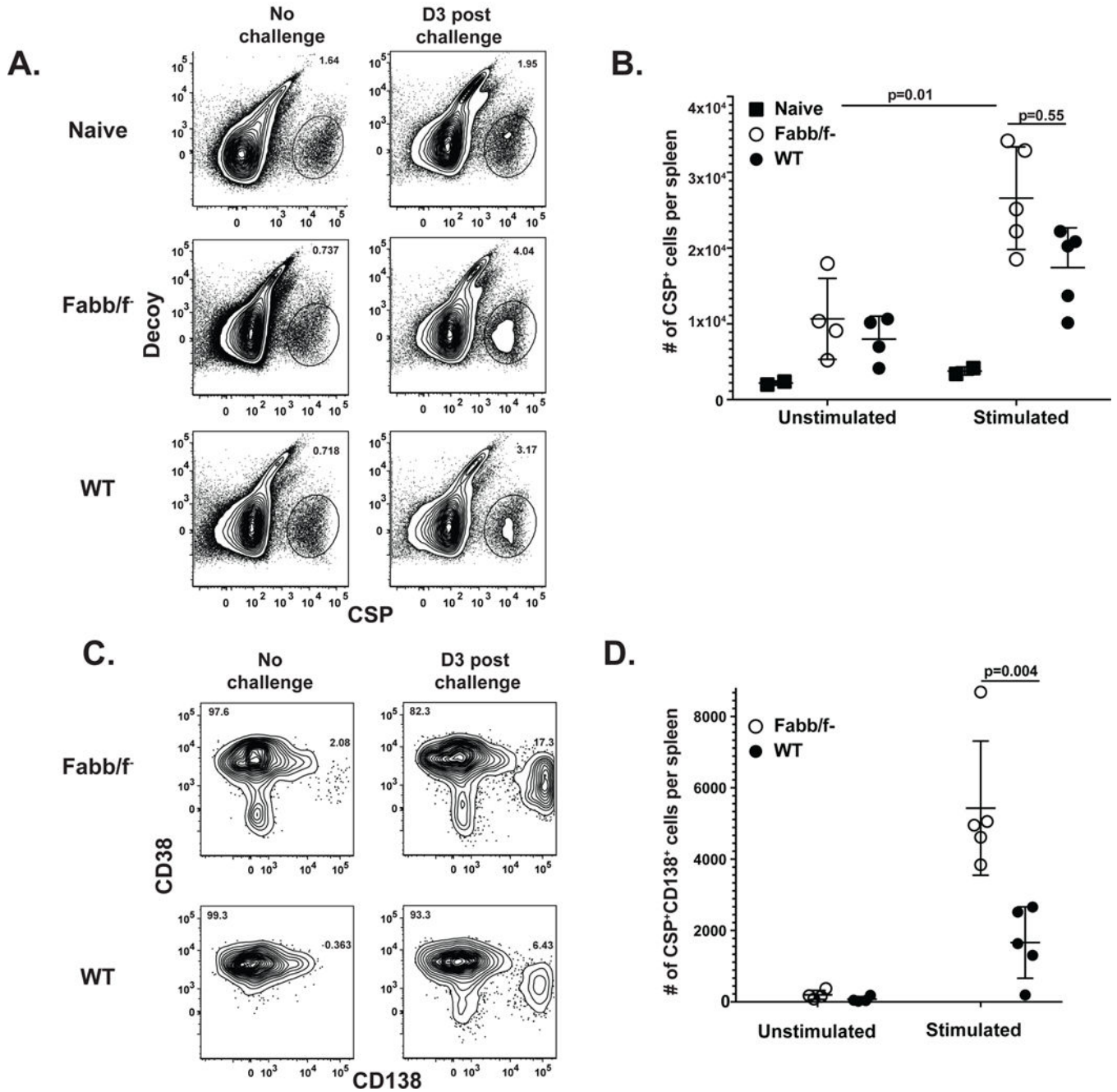


**Figure 5. Blood stage infection impedes secondary response to liver stage antigens**  
 Naïve or Memory mice (day 30) infected with *Pyfabb/f* or *PyWT* sporozoites mice were challenged with 50,000 *Pyfabb/f* sporozoites and *PyCSP* B cells were enriched and analyzed by flow cytometry 3 days later. (A) Representative plots identifying *PyCSP*<sup>+</sup> B cells before and after challenge (B) A summary of total numbers of *PyCSP*<sup>+</sup> B cells presented in (A). (C) Representative plots of plasmablasts (*PyCSP*<sup>+</sup>B220<sup>+</sup>CD38<sup>low</sup>CD138<sup>+</sup>) before and after challenge in memory mice (D) Total number of plasmablasts presented in (C). Data are from two independent experiments with 5 mice per group. Error bars represent SD.

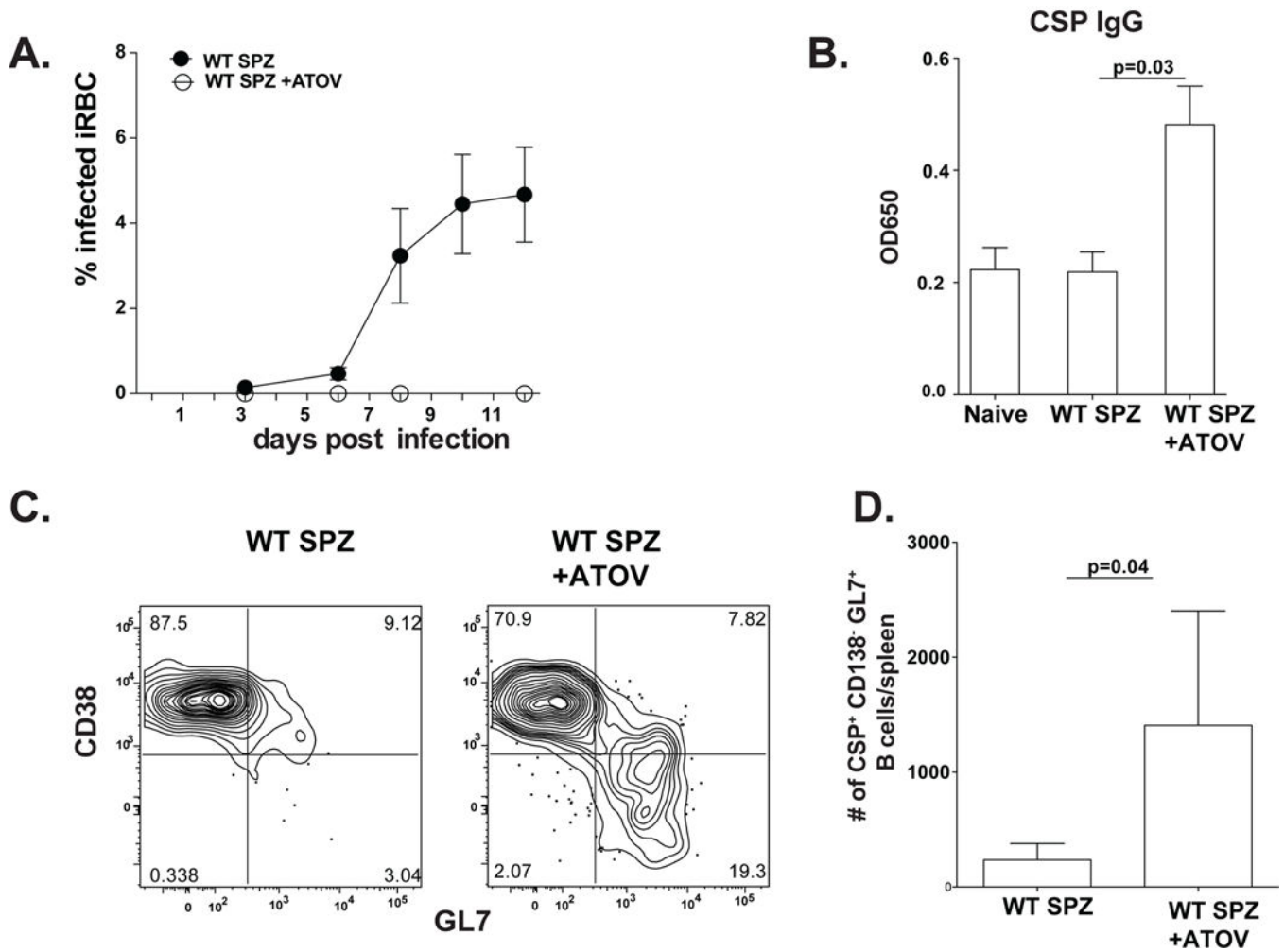


**Figure 6. Drug treatment of WT restores CSP specific responses**

(A) Parasitemia of mice infected with 50,000 PyWT-GFP<sub>Luc</sub> sporozoites with or without treatment with atovoquone from days 3–13, as measured by flow cytometry. (B) Serum was collected from naive or 14 days after infection with or without treatment and anti-*Py*CSP total IgG was measured by ELISA. (C) Splenocytes from *Py*WT infected mice with or without atovoquone treatment were isolated, enriched and analyzed for CSP<sup>+</sup>CD138<sup>-</sup>CD38<sup>-</sup>GL7<sup>hi</sup> germinal center B cells on day 14 by flow cytometry. (D) Graph representing a summary of absolute numbers of CSP<sup>+</sup>CD138<sup>-</sup>CD38<sup>-</sup>GL7<sup>hi</sup> cells presented in C. Results are representative of 2 independent experiments with 4 mice per group. Error bars represent SD. See also figure S2.

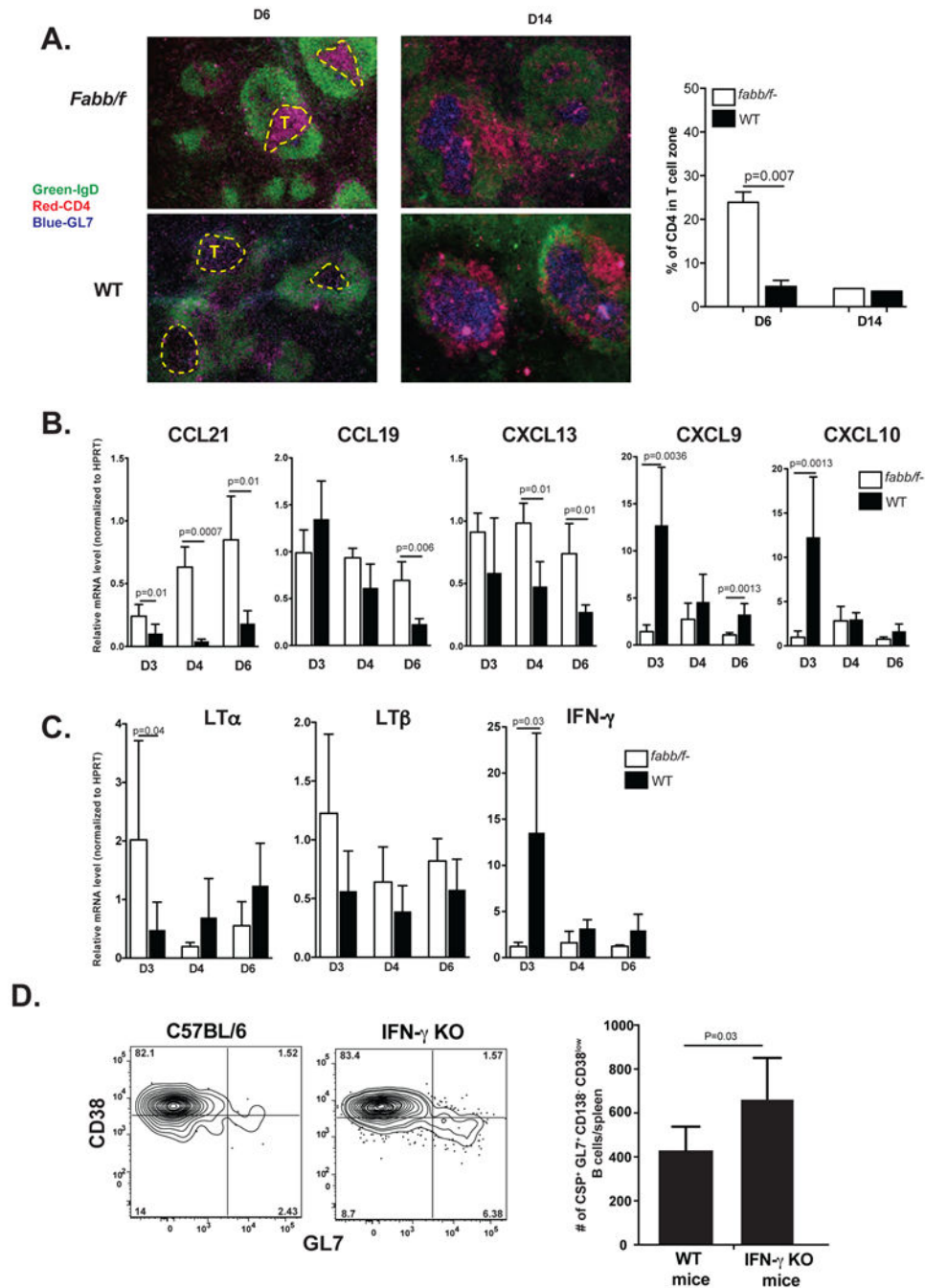


### Figure 7. Blood stages interfere with chemokine expression

(A) Immunofluorescence analysis of spleen sections from mice 6 and 14 days after infection with *Pyfabb/f* or *PyWT* sporozoites. Left panel, B cell follicles were identified with anti-IgD (green), T cells with anti-CD4 (red) and germinal center B cells with anti-GL7 (blue). Yellow dashed lines denote PALS at day 6, white dashed lines denote GCs at day 14. Right panel, quantification of CD4 expression in PALS and GC, expressed as percent of CD4 in PALS or GC to total CD4 signal per field. Images are representative from at least 3 independent experiments. (B and C): Mice were infected with *Pyfabb/f* or *PyWT*

sporozoites and spleens isolated 3, 4 and 6 days later. mRNA levels were analyzed by qRT-PCR. All samples were standardized to the housekeeping gene *hprt* and fold changes were calculated relative to naïve controls (B) Gene expression levels of the chemokines *ccl21*, *ccl19*, *cxcl13*, *cxcl9* and *cxcl10*. (C) Gene expression of regulatory cytokines; *lymphotoxin  $\alpha$* , *lymphotoxin  $\beta$*  and *ifn- $\gamma$* . Data represent 3–6 mice with 2–3 independent experiments. D) Splenocytes from C57BL/6 mice and mice that lack IFN $\gamma$  signaling (IFNGr $^{-/-}$ ) mice were infected with *PyWT* sporozoites, splenocytes were isolated, enriched and analyzed for CSP $^{+}$ CD38 $^{low}$  CD138 $^{-}$  GL7 $^{hi}$  germinal center B cells on day 14 by flow cytometry. Results are representative of 2 independent experiments with 5 mice per group. Error bars represent SD.